Phys. Status Solidi B **252,** No. 6, 1370–1381 (2015) / **DOI** 10.1002/pssb.201451516

physica status solidi b
www.pss-b.com
basic solid state physics

Ballistic conduction in macroscopic non-periodic lattices

Chumin Wang*[,1], Carlos Ramírez[2], Fernando Sánchez[2], and Vicenta Sánchez[2]

[1] Instituto de Investigaciones en Materiales, Universidad Nacional Autónoma de México, Apartado Postal 70-360, 04510 D.F., México
[2] Departamento de Física, Facultad de Ciencias, Universidad Nacional Autónoma de México, Apartado Postal 70-542, 04510 D.F., México

Received 11 September 2014, revised 22 November 2014, accepted 5 January 2015
Published online 9 February 2015

Keywords ballistic conduction, disordered materials, non-periodic lattices, renormalization method

* Corresponding author: e-mail chumin@unam.mx, Phone number: +52 55 5622 4634, Fax number: +52 55 5616 1251

In this paper, the dc electronic transport at zero temperature in aperiodic systems with macroscopic length is studied by using a real-space renormalization plus convolution method developed for the Kubo–Greenwood formula within the tight-binding formalism. We analytically prove the existence of transparent states in several generalized Fibonacci lattices, as well as in segmented linear chains, where they always appear if the number of bonds in each segment is even, regardless the ordering of segments. For two-dimensional square-lattice tapes with a periodic or non-periodic Fano-impurity plane, we found a novel ballistic transport state in the dc conductance spectra.

1 Introduction Electric conductivity is one of the most important properties of solids due to its relevance in the design and construction of new electronic devices, also is one of the most susceptible to the presence of defects. The miniaturization of electronic devices has revealed the importance of quantum effects, such as the ballistic conduction in nanoelectronics when the device length is smaller than the inelastic scattering mean-free-path of very pure materials. According to the Abrahams' theorem [1], all the states are localized in one- and two-dimensional (2D) systems with an infinitesimal random-disorder strength. Recently, it is observed that 2D disordered systems can exhibit dramatic drops in resistivity as the temperature $T \to 0$, suggesting a metallic ground state in such systems [2–4]. On the other hand, delocalized electronic states have been found in one-dimensional (1D) systems with correlated disorder [5–8] and with random dimers [9]. Analytical results by Damanik and Gorodetski prove the possible existence of ballistic transport for Fibonacci Hamiltonian with diagonal disorder when the coupling goes to zero [10]. A more general analysis about the transparent states in aperiodic lattices can be found in Ref. [11].

In general, the presence of structural disorders makes useless the reciprocal space and the analysis of their effects on the electronic transport is usually carried out in small systems or by using the perturbation theory. For example, it has been addressed by computing the scaling behavior of the mean-square displacement of the wave packets with respect to time via a renormalization group approach developed within the Brillouin–Wigner perturbation theory [12]. Other renormalization approaches based on transfer matrices have also been used to address the electronic transport in aperiodic systems [13]. In this paper, we study the ballistic transport in 1D generalized Fibonacci lattices [14, 15] and N-mer segmented chains, both with macroscopic length of 10^8 atoms. The numerical analysis was carried out by means of an exact real-space renormalization method developed for the Kubo-Greenwood formula and the analytical demonstration of transparent states has been performed through the transmittance within the Landauer formalism. For 2D systems, we report for the first time the finding of a ballistic conduction state in conducting tapes with a Fano-impurity plane.

2 The model In this article, we address the bond problem, i.e., systems containing the same type of atoms but different electron hopping integrals between them. Let us consider a cubically structured lattice with two kinds of hopping integrals between nearest neighbor atoms, t_A and t_B, and they are arranged in a non-periodic way. For the periodic case we have $t_A = t_B$ and for aperiodic chains, the hopping integrals are rdered following a generalized Fibonacci sequence (F_k) defined as $F_k = mF_{k-1} \oplus nF_{k-2}$ where $F_0 = \mathrm{A}$ and $F_1 = \mathrm{A}^m\mathrm{B}^n$. For example, $F_3 = \mathrm{AABAABAAABAABAAAB}$ for $m = 2$

and $n=1$. In order to isolate the bond-disorder effects on the physical properties, a single-band tight-binding Hamiltonian with null self-energies is taken,

$$H=\sum_j \left[t_{j,j+1}|j\rangle\langle j+1|+t_{j,j-1}|j\rangle\langle j-1|\right], \tag{1}$$

where $t_{j,k}=\langle j|H|k\rangle$ denotes the hopping integral between nearest-neighbor atoms j and k and $|j\rangle$ are Wannier states.

The electrical conductivity can be calculated within the linear response theory by using the Kubo–Greenwood formula given by [16]

$$\sigma(\mu,\omega,T)=\frac{2e^2\hbar}{\Omega\pi m^2}\int_{-\infty}^{\infty}\mathrm{d}E\frac{f(E)-f(E+\hbar\omega)}{\hbar\omega}\times \mathrm{Tr}[p\,\mathrm{Im}\,G^{+}(E+\hbar\omega)p\,\mathrm{Im}\,G^{+}(E)], \tag{2}$$

where Ω is the volume of the system, $G^{+}(E)=G(E+i\eta)$ is the retarded one-particle Green's function and $f(E)=\{1+\exp[(E-\mu)/k_BT]\}^{-1}$ is the Fermi–Dirac distribution with the Fermi energy μ and temperature T, and p is the projection of the momentum operator along the applied electrical field, which can be expressed in terms of Wannier states as

$$p=\frac{im}{\hbar}[H,x]=\frac{ima}{\hbar}\sum_j\left\{t_{j,j+1}|j\rangle\langle j+1|-t_{j-1,j}|j\rangle\langle j-1|\right\}, \tag{3}$$

for systems with a constant lattice parameter (a) and the structural disorder is introduced through the arrangement of hopping integrals. For the case of a periodic chain connected to two semi-infinite periodic leads, the zero-temperature dc conductivity is [8]

$$\sigma_P=\sigma(E,0,0)=\frac{e^2a}{\pi\hbar}(N-1), \tag{4}$$

where $(N-1)a$ is the system length.

In general, the electrical conductance (g) of a two-dimensional lattice can be written as

$$g(\mu,\omega,T)=\sigma^{2D}(\mu,\omega,T)\Omega_{\perp}/\Omega_{\parallel}, \tag{5}$$

where $\Omega_{\parallel}$ and $\Omega_{\perp}$ are the volumes of parallel and perpendicular subspaces, respectively. The electrical conductivity of cubically structured two-dimensional lattices (σ^{2D}) can be calculated by using the convolution theorem [17]

$$\sigma^{2D}(\mu,\omega,T)=\sum_{\beta}\sigma(\mu-E_{\beta},\omega,T), \tag{6}$$

where E_{β} are the eigenvalues of the perpendicular subspace. There is a natural unit of the electrical conductance given by $g_0=2e^2/h$. All the systems analyzed in this article are connected to two semi-infinite periodic leads with hopping integrals t and null self-energies, and we always take $t_B=t$.

3 Generalized Fibonacci chains Ballistic conduction is the electronic transport without scattering having unit transmittance, called transparent states, whose electrical conductivity is $\sigma=\sigma_p$. In this section we analyze the existence of transparent states in generalized Fibonacci chains (GFC) characterized by (m,n), whose numbers of atoms in the studied systems are summarized in Table 1.

The zero-temperature dc conductivity spectra $[\sigma(\mu,0,0/\sigma_p)]$ around $\mu=0$ in color scale are shown in Fig. 1 as a function of the chemical potential (μ) and the hopping integral t_A for GFC indicated in Table 1, where the imaginary part of energy is $\eta=10^{-15}|t|$. The systems with $n=1$, corresponding to Fig. 1(a–d), have a transparent state at $\mu=0$ every two generations if m is even and every six generations if m is odd. For these quasiperiodic systems, when the disorder strength $\gamma\equiv t_A/t_B\to 0$, the electrical conductivity also tends to zero except for $\mu=0$. For GFC with $n=2$, Fig. 1(e–h), we always find a transparent state at $\mu=0$ for all the generations with even numbers of m. Around this transparent state the conductivity spectra have an oscillating behavior. In contrast, we never find a transparent state at $\mu=0$ if $n=2$ and m is odd. For GFC with $n=3$, shown in Fig. 1(i–l), we find transparent states every two generations when m is even and a gap around $\mu=0$ when m is odd. In general, there is a notable similarity between the conductivity spectra of $n=2$ and of $n=4$, and both decay slower than those corresponding to $n=1$ when γ goes to zero.

Figure 2 shows the high conductivity peaks with $\sigma(\mu,0,0)\geq 0.999999999999\sigma_p$ in the space of the chemical potential (μ) and hopping integral ratio t_A/t_B for the GFC of Table 1. Notice that we recover the transparent states observed in Fig. 1. Additionally, we can see many extreme high conductivity states located at $\mu/|t|=\pm t_A/t_B$ for GFC with $n=3$ and $m=3$, as well as at $\mu/|t|=\pm 0.71t_A/t_B$ for $n=4$ and $m=4$. In Fig. 3, $\sigma(\mu=0,0,0)$ versus the generation number (k) in 16 types of GFC are shown for

Table 1 Number of atoms (N) and generation number (k) of analyzed GFC (m,n).

N	$n=1$	$n=2$	$n=3$	$n=4$
$m=1$	433494438 ($k=42$)	357913942 ($k=29$)	315732482 ($k=24$)	235418370 ($k=21$)
$m=2$	768398402 ($k=24$)	268377089 ($k=20$)	1743392202 ($k=20$)	234029057 ($k=17$)
$m=3$	790171310 ($k=18$)	253841390 ($k=16$)	712268722 ($k=16$)	429496730 ($k=15$)
$m=4$	165580142 ($k=14$)	352738177 ($k=14$)	678529304 ($k=14$)	250597377 ($k=13$)

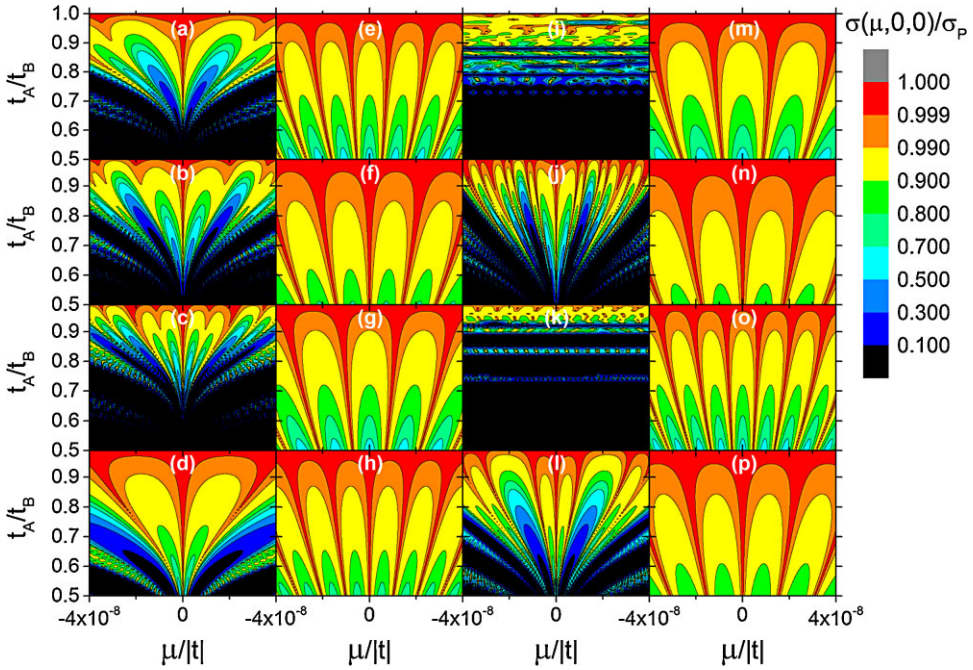

Figure 1 Electrical conductivity (σ) in color scale as a function of the chemical potential (μ) and the hopping integral ratio t_A/t_B for generalized Fibonacci chains (GFC) with (m,n) equal to (a) (1,1), (b) (2,1), (c) (3,1), (d) (4,1), (e) (1,2), (f) (2,2), (g) (3,2), (h) (4,2), (i) (1,3), (j) (2,3), (k) (3,3), (l) (4,3), (m) (1,4), (n) (2,4), (o) (3,4), (p) (4,4), whose system lengths are specified in Table 1.

$t_A = 0.8t_B$ (red solid circles) and $t_A = 0.5t_B$ (blue open circles). For instance, the transparent states appear every six generations in Fig. 3(a) and 3(c), every two generations in Fig. 3(b), 3(d), 3(j) and 3(l), and they are present in all the generations of Fig. 3(f), 3(h), 3(p) and 3(r). Finally, there is not transparent state at $\mu = 0$ in Fig. 3(e), 3(g), 3(i), 3(k), 3(o) and 3(q). Analytical proofs of these transparent states will be presented in the next section.

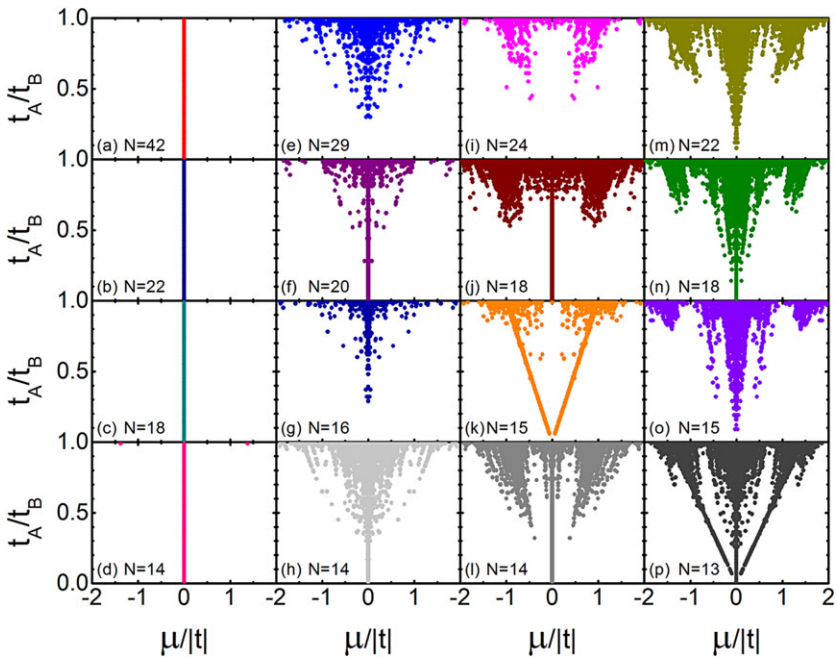

Figure 2 High conductivity states with $\sigma(\mu,0,0) \geq 0.999999999999\sigma_p$ as a function of the chemical potential (μ) and the hopping integral t_A for the GFC specified in Table 1.

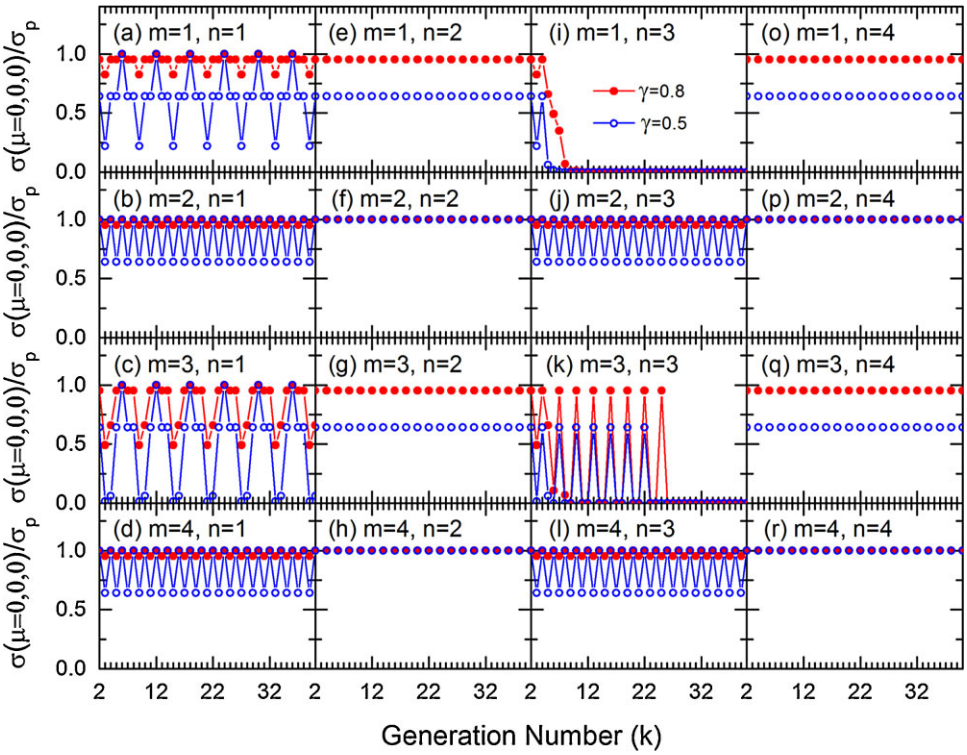

Figure 3 DC conductivity at $\mu = 0$ as a function of the generation number (k) for GFC with $t_A = 0.8t_B$ (red solid circles) and $t_A = 0.5t_B$ (blue open circles).

4 Analytical results An alternative way to calculate the electrical conductivity in one-dimensional systems is by means of the Landauer formula given by $\sigma_L(\mu) = \sigma_P T$, where T is the transmittance [18]. The stationary Schrödinger equation for Hamiltonian (1) can be rewritten as

$$\begin{pmatrix} c_{j+1} \\ c_j \end{pmatrix} = \mathbf{T}_j \begin{pmatrix} c_j \\ c_{j-1} \end{pmatrix} = \begin{pmatrix} \dfrac{\mu}{t_{j,j+1}} & \dfrac{t_{j,j-1}}{t_{j,j+1}} \\ 1 & 0 \end{pmatrix} \begin{pmatrix} c_j \\ c_{j-1} \end{pmatrix}, \quad (7)$$

Table 2 Transmittance of eight GFC of type (m,n) for generation $k \geq 3$.

(m,n)	$\tau_{i,j}$	transmittance $[T(\mu = 0)]$
(2,2) (2,4) (4,4)	$\tau_{i,j}(k) = \begin{cases} (-1)^i & \text{if } i \neq j \\ 0 & \text{if } i = j \end{cases}$	1
(4,2)	$\tau_{i,j}(k) = \begin{cases} (-1)^j & \text{if } i \neq j \\ 0 & \text{if } i = j \end{cases}$	
(2,1) (4,3)	$\tau_{i,j}(k) = \begin{cases} s\gamma^{p(k)(-1)^i} & \text{if } i = j \\ 0 & \text{if } i \neq j \end{cases}$	$\dfrac{4}{[\gamma^{p(k)} + \gamma^{-p(k)}]^2}$
(2,3) (4,1)	$\tau_{i,j}(k) = \begin{cases} -\gamma^{p(k)(-1)^i} & \text{if } i = j \\ 0 & \text{if } i \neq j \end{cases}$	

where $\mathbf{T}_j$ is the transfer matrix and c_j is he amplitude of the wavefunction at site j. For chains connected to two semi-infinite periodic leads with hopping integrals t and null self-energies, the transmittance (T) in terms of the product of transfer matrixes, with elements $\tau_{i,j} = (\prod_{s=1}^{N} \mathbf{T}_s)_{i,j}$, is given by [18]

$$T(\mu) = \frac{4 - (\mu/t)^2}{\left[\tau_{2,1} - \tau_{1,2} + (\tau_{2,2} - \tau_{1,1})\mu/2t\right]^2 + (\tau_{2,2} + \tau_{1,1})^2(1 - \mu^2/4t^2)}. \quad (8)$$

For the states at $\mu = 0$ of eight (m,n)-type GFC, the elements $\tau_{i,j}$ are given in Table 2, where $p(v) = [(-1)^v - 1]/2$. Notice that there is a transparent state for all the generations in the first four GFC in Table 2, while transparent states at $\mu = 0$ appear in the last four GFC only if the generation is even. In particular, the elements $\tau_{i,j}$ for (2,2)-type GFC are explicitly obtained in Appendix A.

In addition to those GFC presented in Table 2, we also obtained analytical results for GFC with $m = n = 1$ and generation k, whose elements $\tau_{i,j}$ are

$$\tau_{i,j}(k) = -vf(i+j)[p(v)\theta(k)\gamma^{[1+\theta(k)]\theta(i)} + f(v)\gamma^{\theta(i)}] - (j-i)\theta(k)\left(1 - \left\lceil \frac{v}{2} \right\rceil\right)\gamma^{\theta(k)(j-i)}, \quad (9)$$

which leads to

$$T(0) = 4\left[f(v)(\gamma+\gamma^{-1})^2 + [1-(-1)^v]\right.$$
$$\left.\times\{\gamma^{1+\theta(k)} + \gamma^{-[1+\theta(k)]}\}^2/2\right]^{-1}, \quad (10)$$

where $f(v) = [1+(-1)^v]/2$, $v = (k-2) \bmod (3) \in [0,2]$ and $\theta(i) = (-1)^{i+1}$. Also, for GFC of generation k with $(m,n) = (3,1)$,

$$\tau_{i,j}(k) = -vf(i+j)\left[p(v)\gamma^b + \frac{f(v)}{2}\theta(k)\gamma^{\theta(i)d}\right]$$
$$-\gamma^{-\theta(c)|j-i|}\left\lceil\frac{1-v}{2}\right\rceil\theta(c) \quad (11)$$

and the transmittance at $\mu = 0$ is

$$T(0) = 4\left\{\left(\left\lceil\frac{1-v}{2}\right\rceil\right)^2(\gamma+\gamma^{-1})^2\right.$$
$$+v^2\left[-p(v)\left(\gamma^{-2[1+\theta(k)]} + \gamma^{2[1+\theta(k)]}\right)\right.$$
$$\left.\left.+\frac{f(v)(\gamma^d+\gamma^{-d})}{2}\right]\right\}^{-2}, \quad (12)$$

where $b = -4\theta(i)p(k)$, $c = k+1-j$ and $d = 3f(k) - p(k)$. Equations (10) and (12) indicate that these GFC present a transparent state at $\mu = 0$ every six generations.

5 Segmented chains For a periodic chain with one and two segment defects as respectively shown in Fig. 4(a) and 4(b), each segment contains two hopping integrals t_A while the periodic chain is formed by hopping integrals $t_B = t$.

For the case of a single segment impurity as shown in Fig. 4a, the analytic solution of Landauer conductivity through transmittance (8) is obtained,

$$\sigma_L(\mu) = \frac{4-(\mu/t)^2}{4t_A^2 - \mu^2(2+\gamma^{-2})}t_A^2\sigma_P, \quad (13)$$

whose conductivity spectrum in color scale versus the chemical potential (μ) and the hopping integral t_A is shown in Fig. 5a. Observe that when $t_A \to 0$ but $t_A \neq 0$ the whole conductivity spectrum tends to zero except for $\mu = 0$, where a unique transparent state is found as indicated in Eq. (13). When we have two segment defects separated by N segments as shown in Fig. 4b, the analytic solution of conductivity becomes

$$\sigma_L(\mu) = \frac{\left[4-(\mu/t)^2\right]\sigma_P}{4 - \frac{\mu^2}{t^2} + \frac{\mu^2(t_A^2-t^2)^2}{t_A^8 t^4}\left[\mu^2\left(2t_A^2+t^2-\mu^2\right)^2 - \rho(\mu)\frac{\tau_{11}^2(N-1)}{t^2} - \vartheta(\mu)\frac{\mu\tau_{11}(N-1)\tau_{11}(N-2)}{t}\right]}, \quad (14)$$

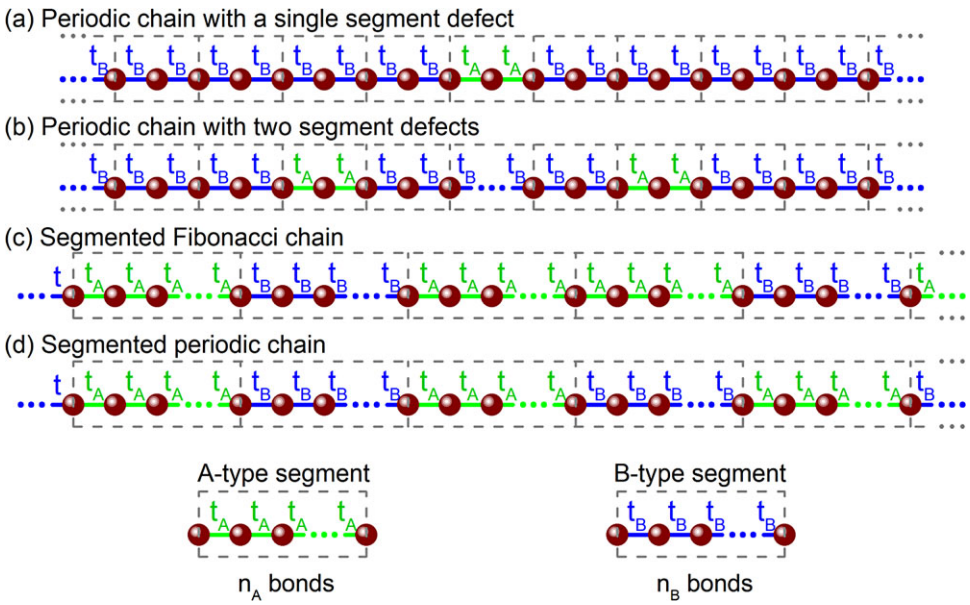

Figure 4 Schematic representations of periodic chains with (a) one and (b) two A-type segment defects, (c) segmented Fibonacci and (d) segmented periodic chains.

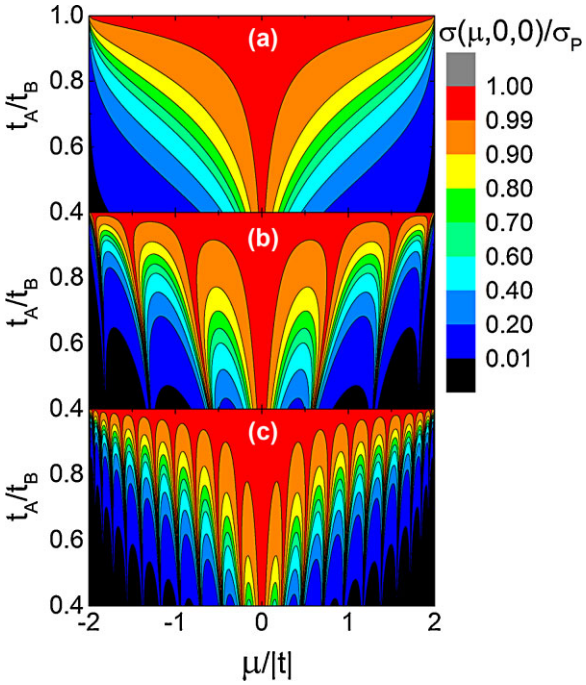

Figure 5 DC conductivity (σ) in color scale as functions of the chemical potential (μ) and the hopping integral t_A in segmented chains with (a) a single segment defect and two segment defects separated by (b) four and (c) ten segments.

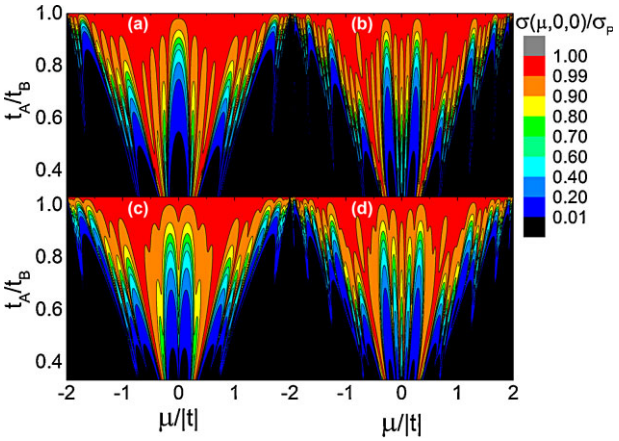

Figure 6 DC conductivity (σ) in color scale as functions of the chemical potential (μ) and the hopping integral t_A for segmented chains ordered periodically as ABABABABA with (a) $n_B = 9$ and (b) $n_B = 24$ or quasiperiodically as ABAABABA with (c) $n_B = 9$ and (d) $n_B = 24$, where $n_A = 3$ in all the cases.

where $\rho(\mu) = \mu^2 t^2 \left(12t_A^4 + 12t_A^2 t^2 + t^4\right) - \mu^4 \left(4t_A^4 + 16t_A^2 t^2 + 6t^4\right) + \mu^6 \left(4t_A^2 + 5t^2\right) - 4t_A^4 t^4 - \mu^8$, $\vartheta(\mu) = \mu^2 \left(4t_A^4 + 12t_A^2 t^2 + 3t^4\right) - 4\mu^4 \left(t^2 + t_A^2\right) - 4t_A^2 \left(2t_A^2 t^2 + t^4\right) + \mu^6$ and $\tau_{11}(N) = \sum_{l=0}^{[N/2]} (-1)^l (N-l)!(\mu/t)^{N-2l}/[l!(N-2l)!]$. From Eq. (14) we obtain the electrical conductivity spectra in color scale versus the chemical potential (μ) and the hopping integral t_A, as illustrated in Fig. 5(b) and 5(c) respectively for the cases of two segment defects separated by four and ten segments. Notice that a transparent state at $\mu = 0$ is present for any separation of the two segment defects, as shown in Eq. (14). In contrast to the case of a single segment defect, the spectra of two segment defects present oscillations along μ, whose frequency is larger when the separation between segment defects grows.

Let us now consider a segmented chain composed by two kind of segments. The first ones contain n_A bonds with hopping integral t_A and the others contain n_B bonds with hopping integral t_B. These segments can be placed following periodic or quasiperiodic orderings. In Fig. 6, dc conductivity spectra in color scale versus the chemical potential (μ) and the hopping integral t_A are shown for segmented chains composed by five A-type segments ($N_A = 5$) with $n_A = 3$, separated from each other by B-type segments with (a) $n_B = 9$ and (b) $n_B = 24$, i.e., constructing the segmented chain as ABABABABA. In Fig. 6c and d, the segments are ordered following the Fibonacci sequence ABAABABA with $n_B = 9$ and $n_B = 24$, respectively. In all the cases we have $n_A = 3$ and the segmented chains are connected to two semi-infinite periodic leads with hopping integrals t. Observe that these segmented chains do not possess a transparent state at $\mu = 0$, because the number of bonds in A-type segment ($n_A = 3$) is odd and the number of A-type segments ($N_A = 5$) is also odd, as will be shown in Eq. (15). Moreover, the B-type segment length and the segment ordering determine the position of high conductivity peaks.

Figure 7 shows the conductivity spectra of the same systems as in Fig. 6, except that the lengths of segments are now $n_A = 8$ and (a) $n_B = 8$, (c) $n_B = 8$, (b) $n_B = 64$, and (d) $n_B = 64$. Observe the existence of a transparent state at $\mu = 0$, for both periodic and quasiperiodic ordering, as well as both B-type segment lengths. In fact, there is a general

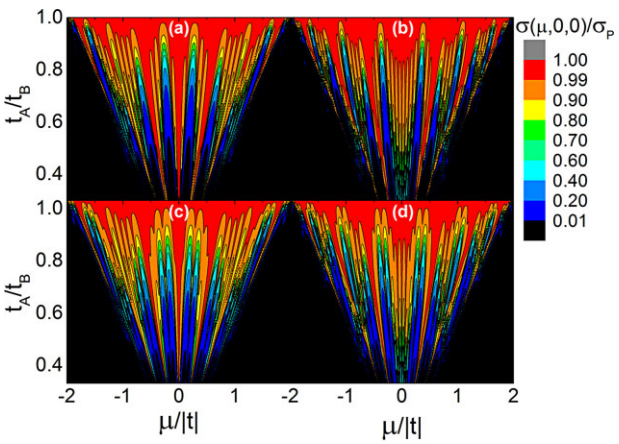

Figure 7 DC conductivity (σ) in color scale as a function of the chemical potential (μ) and the hopping integral t_A for segmented chains ordered periodically as ABABABABA with (a) $n_B = 8$ and (b) $n_B = 64$ or quasiperiodically as ABAABABA with (c) $n_B = 9$ and (d) $n_B = 64$, where $n_A = 8$ in all the cases.

theorem about the existence of a transparent state at $\mu = 0$ in a chain of N atoms connected to two semi-infinite periodic leads if

$$\prod_{l=1}^{\lfloor N/2 \rfloor} \frac{t_{2l,2l-1}}{t_{2l,2l+1}} = 1 \tag{15}$$

as demonstrated in Appendix B. From Eq. (15), for instance, if the number of bonds in all the segments is even, there is always a transparent state at $\mu = 0$ regardless the number and ordering of segments neither the value of hopping integrals. In contrast, if n_A and N_A are both odd, there is no transparent state at $\mu = 0$.

In the next section, we extend the analysis to two-dimensional tapes with a Fano impurity plane.

6 Multidimensional systems For a two-dimensional cubically-structured tape with a single Fano impurity plane as shown in Fig. 8, the Hamiltonian given by Eq. (1) is separable and then the convolution theorem (6) can be used to calculate its conductance. In this section, we prove that such tapes with null self-energies and constant hopping integral have a transparent state at $\mu = 0$ if their width is equal to the Fano impurity length minus two bonds. In fact, this proof can also be applied to tapes with aperiodic transversal section when the Fano impurity has the same aperiodicity, regardless the nature of the first two connecting bonds.

For periodic chains with an attached periodic Fano impurity chain of N_F atoms, both formed by hopping integrals t, there are transparent states at the eigenvalues of a (N_F-1)-atom periodic chain [19]. In general, the Landauer conductivity of a periodic chain with a coupled Fano impurity chain of arbitrary hopping integrals is shown in Appendix C to be

$$\sigma_L(\mu) = \frac{4 - (\mu/t)^2}{4 - (\mu/t)^2 + t_{N_F}^4 \beta_{N_F-1}^2(\mu)/[t^2 \beta_{N_F}^2(\mu)]} \sigma_P, \tag{16}$$

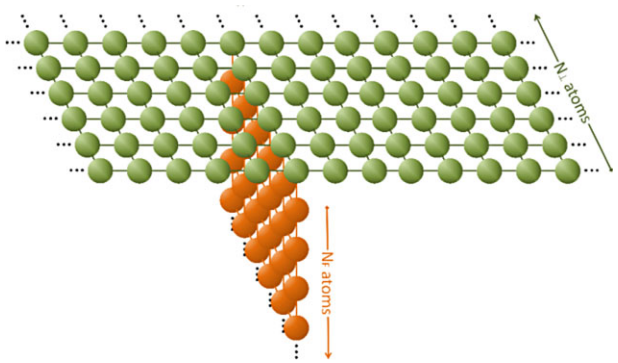

Figure 8 Schematic representation of a two-dimensional periodic tape of infinite length and a width of $N_\perp$ atoms (green balls) with an attached Fano impurity plane of $N_F N_\perp$ atoms (orange balls).

which becomes σ_P when $\beta_{N_F-1}(\mu) = 0$, where

$$\beta_N(\mu) \equiv \det \begin{pmatrix} \mu & -t_1 & 0 & \cdots & 0 \\ -t_1 & \mu & -t_2 & \ddots & \vdots \\ 0 & -t_2 & \mu & \ddots & 0 \\ \vdots & \ddots & \ddots & \ddots & -t_{N-1} \\ 0 & \cdots & 0 & -t_{N-1} & \mu \end{pmatrix}. \tag{17}$$

By using the convolution theorem of Eq. (6), the conductivity of two-dimensional periodic tapes with a Fano impurity plane (σ^{2D}) can be obtained from Eq. (16),

$$\sigma^{2D}(\mu,0,0) = \sum_\beta \frac{4 - [(\mu - E_\beta)/t]^2}{4 - [(\mu - E_\beta)/t]^2 + t_{N_F}^4 \beta_{N_F-1}^2(\mu - E_\beta)/[t^2 \beta_{N_F}^2(\mu - E_\beta)]} \sigma_P, \tag{18}$$

where E_β are the eigenenergies of the perpendicular subspace of $N_\perp$ atoms. If the hopping integrals in the transversal section are t_1,t_2, $\cdots$, and t_{N_F-2}, all E_β become solution of $\beta_{N_F-1}(E_\beta) = 0$ and then

$$\sigma^{2D}(\mu = 0,0,0) = N_\perp \sigma_P, \tag{19}$$

showing the existence of a ballistic state at $\mu = 0$ in a two-dimensional tape with a Fano impurity plane. In fact, if the self-energies of the Fano impurity plane are ε_F, this ballistic conduction state would be at $\mu = \varepsilon_F$.

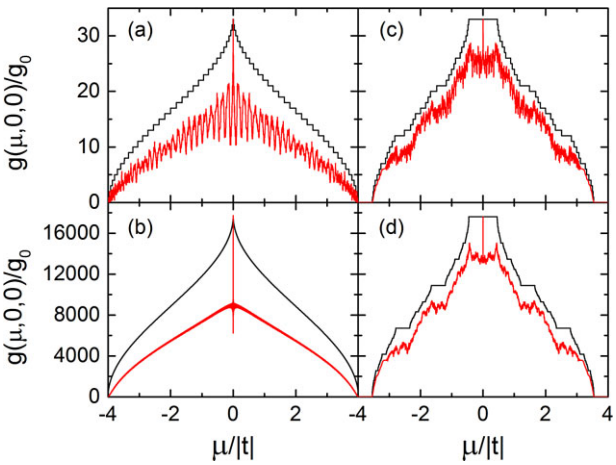

Figure 9 Electrical conductance (g) as a function of the chemical potential (μ) for the system of Fig. 8, whose transversal section has (a) $N_\perp = 33$ and (b) $N_\perp = 17710$ atoms following a periodic sequence or (c) $N_\perp = 33$ and (d) $N_\perp = 17710$ atoms following the Fibonacci sequence with $t_A = t(\sqrt{5} - 1)/2$, for $N_F = N_\perp + 1$ (red lines) and $N_F = 0$ (black lines).

Figure 9 shows the electrical conductance spectrum (g) versus the chemical potential (μ) of two-dimensional tapes with a Fano impurity plane as illustrated in Fig. 8, whose transversal section is periodic with (a) 33 atoms and (b) 17710 atoms, or is quasiperiodic with (c) 33 atoms and (d) 17710 atoms. The black lines show the conductance of tapes without Fano defects and the red lines display g of tapes with $N_F = N_\perp + 1$ where the hopping integrals along the Fano impurity plane follow the same ordering as in the transversal section. In all quasiperiodic systems of Fig. 9 $t_A = t(\sqrt{5}-1)/2$ is taken. Observe the step pattern in electrical conductance spectra for systems without Fano impurities, such behavior have been experimentally confirmed by Ron and Dagan [20]. In particular, there is a ballistic wide zone around $\mu = 0$ for periodic tapes with quasiperiodic transversal sections and the width of such zone grows when t_A diminishes. In general, the conductance of these tapes is larger than that obtained from tapes with periodic transversal section and the same $N_\perp$, because that a smaller hopping integral in the perpendicular subspace causes lower interference between conducting channels. Moreover, there is a ballistic state at $\mu = 0$ as expected from Eq. (19).

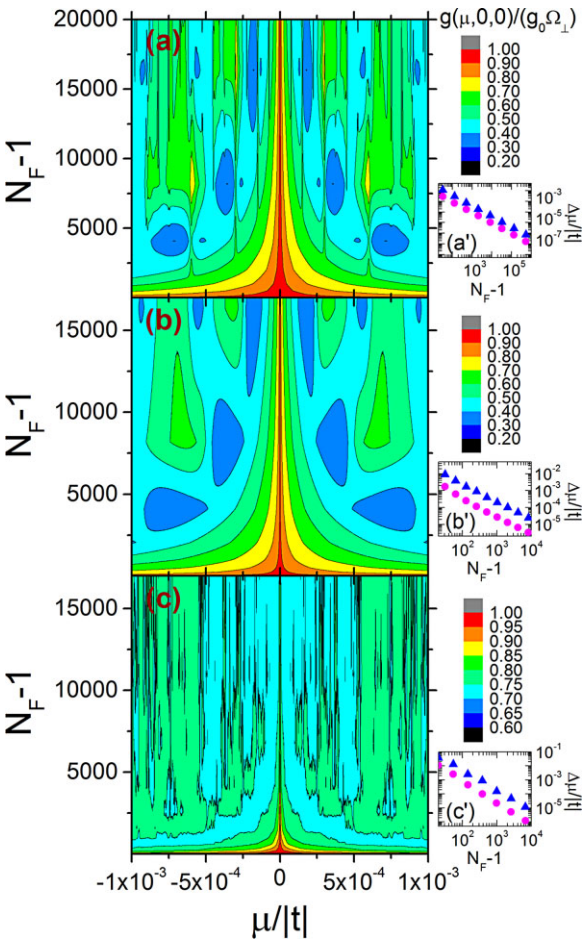

Figure 10 Amplification of the conductance spectra (g) around $\mu = 0$ in color scale as functions of the chemical potential (μ) and the number of atoms along the Fano defect (N_F) for (a) $N_\perp = 15$, (b) $N_\perp = N_F - 1$ with hopping integrals in the Fano impurity plane and transversal section following the periodic sequence and (c) $N_\perp = N_F - 1$ for such hopping integrals following the Fibonacci sequence. Insets: Width of the ballistic conductance peak versus N_F measured at $g(\mu,0,0) = 0.9N_\perp g_0$ (solid magenta circles) and $g(\mu,0,0) = 0.8N_\perp g_0$ (solid blue triangles).

In fact, if the eigenvalues of the transversal section (E_β) are a subset of the solutions of $\beta_{N_F-1}(E) = 0$, there is ballistic conductance at $\mu = 0$. For example, in systems of Fig. 8 with all hopping integrals t we find such ballistic conduction if $N_F = 2^p(N_\perp+1)$, being p a positive integer number. Figure 10 shows in color scale a magnification of the conductance spectra around the ballistic conduction peak at $\mu = 0$ as a function of the Fano impurity length (N_F), for the cases of (a) all the hopping integrals t, $N_\perp = 15$ and $N_F = 2^p(N_\perp + 1)$, and the hopping integrals following (b) periodic and (c) Fibonacci sequence with $N_\perp = N_F - 1$. In insets 10(a'–c') we plot the width of the ballistic conductance peak measured at $g(\mu,0,0) = 0.9N_\perp g_0$ (solid magenta circles) and $g(\mu,0,0) = 0.8N_\perp g_0$ (solid blue triangles).

Observe in the insets of Fig. 10 that the widths of ballistic conductance peaks ($\Delta\mu$) decrease with the length of Fano impurity plane. This fact can be understood by considering that the two-dimensional ballistic conductance peak is a sum of many one-dimensional ballistic peaks and its width is related to the averaged width over one-dimensional ballistic peaks, which decreases with the length of Fano impurity. In addition, Insets 10(a'–c') reveal $\Delta\mu/|t| \approx CN_\perp^{-1}$ and C depends on the cutting level at a given value of the conductance.

7 Conclusions In this paper, we have studied analytically and numerically the ballistic conduction in one- and two-dimensional non-periodic macroscopic lattices with bond disorder in the tight-binding formalism by using a real-space renormalization plus convolution method developed for the Kubo–Greenwood formula.

In one-dimensional systems, for hopping integrals following the generalized Fibonacci sequences characterized by (m,n), we found transparent states at $\mu = 0$ for $n = 1$ and every two generations if m is even or every six generations if m is odd. These chains are quasiperiodic since they accomplish the Pisot conditions and the unimodular substitution matrix [21]. For GFC with $n \neq 1$, there is a transparent state at $\mu = 0$ for all the generations if n and m are both even and every two generations if n is odd and m is even. We also found high conduction with $\sigma(\mu,0,0) \geq 0.999999999999\sigma_p$ at $\mu = \pm t_A$ for GFC with $n = m = 3$ or 4. These transparent states were confirmed in analytical way.

For the case of segmented chains, based on the numerical results we demonstrated analytically in appendix B that if the segments are composed by an even number of bonds there is always a transparent state at $\mu = 0$. This analytical result also ensures other possibilities to obtain transparent states at $\mu = 0$, for example, in chains with two kinds of segment when one of them has an odd number of

bonds, the other has an even number, and the chain contains an even number of the first kind of segment. These affirmations are true for any possible segment ordering and values of hopping integrals. This is a generalization of the Dunlap finding about the apparition of transparent states in any dimer-composed chain [9].

For two-dimensional systems, we proved that infinite periodic tapes with a single periodic Fano impurity plane have a ballistic conductance peak at $\mu = 0$ if the eigenvalues of the transversal subspace are a subset of those obtained from a periodic chain with one atom less than the Fano impurity length. Furthermore, there is transparent state at $\mu = 0$ for any values of hopping integrals along the Fano impurity plane if the transversal section with one atom less than the Fano impurity has the same sequence of hopping integrals. The analysis of the ballistic-peak width reveals a power law decay with the Fano impurity length. In fact, we can move the location of transparent state in the conductance spectra by changing the self-energies of Fano defect. Experimentally, the chemical potential position in the band structure of a nanowire can be modified by an applied gate voltage [22]. This finding of ballistic conduction in multidimensional lattices with Fano impurities could be relevant for the design and understanding of branched nanowires [23].

Appendix A In this appendix, we prove the matrix elements $\tau_{i,j}$ of Table 2 for the case of a generalized Fibonacci chain (GFC) with $(m = 2, n = 2)$. The generation k of this GFC is built through $F_k = F_{k-1} \oplus F_{k-1} \oplus F_{k-2} \oplus F_{k-2}$ with initial conditions of $F_1 = \mathrm{AABB}$ and $F_2 = \mathrm{AABBAABBAA}$. For example, the GFC with $k = 1$ consists of five atoms and four bonds. In general, the GFC is connected to two semi-infinite periodic leads with hopping integrals $t = t_B$ at its both ends, as schematically shown in Fig. 11 Hence, the product of transfer matrixes is

$$\tau_{i,j} = \left(\prod_{s=1}^{N} \mathbf{T}_s\right)_{i,j} = [\mathbf{M}_{\mathrm{R}}(k)\mathbf{M}(k)\mathbf{M}_{\mathrm{L}}(k)]_{i,j}, \qquad \text{(A1)}$$

where $\mathbf{M}_{\mathrm{L}}(k)$ $[\mathbf{M}_{\mathrm{R}}(k)]$ is the transfer matrix of the connection between the GFC and the left [right] lead, and $\mathbf{M}(k)$ is the product of transfer matrixes associated to inside atoms in GFC.

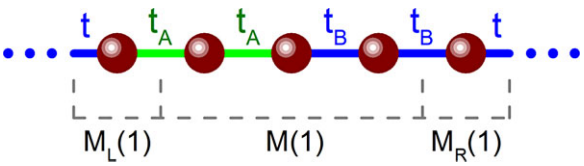

Figure 11 Schematic representation of a (2,2)-type GFC of generation $k = 1$ connected to two semi-infinite periodic leads with hopping integral t. $\mathbf{M}_{\mathrm{L}}(1)$, $\mathbf{M}(1)$ and $\mathbf{M}_{\mathrm{R}}(1)$ are respectively the transfer matrixes associated to the left end, middle atoms and the right end of the GFC.

For example, for $\mu = 0$ we have

$$\mathbf{M}_{\mathrm{L}}(1) = \begin{pmatrix} 0 & -t/t_A \\ 1 & 0 \end{pmatrix}, \quad \mathbf{M}_{\mathrm{R}}(1) = \begin{pmatrix} 0 & -t_B/t \\ 1 & 0 \end{pmatrix}, \qquad \text{(A2)}$$

and

$$\mathbf{M}(1) = \begin{pmatrix} 0 & -1 \\ 1 & 0 \end{pmatrix}\begin{pmatrix} 0 & -t_A/t_B \\ 1 & 0 \end{pmatrix}\begin{pmatrix} 0 & -1 \\ 1 & 0 \end{pmatrix} = \begin{pmatrix} 0 & 1 \\ -t_A/t_B & 0 \end{pmatrix}. \qquad \text{(A3)}$$

Hence, $\tau_{i,j} = (-1)^i(1 - \delta_{i,j})$. By straightforward calculation, we obtain

$$\mathbf{M}(2) = \begin{pmatrix} 0 & -1 \\ 1 & 0 \end{pmatrix}, \quad \mathbf{M}(3) = \begin{pmatrix} 0 & 1 \\ -t_A/t_B & 0 \end{pmatrix} \quad \text{and} \quad \mathbf{M}(4) = \begin{pmatrix} 0 & 1 \\ -1 & 0 \end{pmatrix}. \qquad \text{(A4)}$$

In general, for an electron incident from the left side of GFC we have

$$\mathbf{M}(k) = \mathbf{M}(k-2)\mathbf{U}(k-2)\mathbf{M}(k-2)\mathbf{U}(k-1) \times \mathbf{M}(k-1)\mathbf{U}(k-1)\mathbf{M}(k-1), \qquad \text{(A5)}$$

where

$$\mathbf{U}(k) = \begin{pmatrix} 0 & -\dfrac{[1-(-1)^k]t_B + [1+(-1)^k]t_A}{2t_A} \\ 1 & 0 \end{pmatrix} \qquad \text{(A6)}$$

is the transfer matrix of the union between the end of F_k and the initio of any GFC, which starts always with a hopping integral t_A.

Let us assume that for $k \geq 3$

$$\mathbf{M}(k) = \begin{pmatrix} 0 & 1 \\ -(t_A/t_B)^{[1-(-1)^k]/2} & 0 \end{pmatrix}. \qquad \text{(A7)}$$

The cases $k = 3$ and $k = 4$ are proved in Eq. (A4). By noticing that

$$\mathbf{U}(k)\mathbf{M}(k) = \begin{pmatrix} 0 & -\dfrac{[1-(-1)^k]t_B + [1+(-1)^k]t_A}{2t_A} \\ 1 & 0 \end{pmatrix} \times \begin{pmatrix} 0 & 1 \\ -(t_A/t_B)^{[1-(-1)^k]/2} & 0 \end{pmatrix} = \begin{pmatrix} 1 & 0 \\ 0 & 1 \end{pmatrix}, \qquad \text{(A8)}$$

we obtain immediately that

$$\mathbf{M}(k+1)=\mathbf{M}(k-1)\mathbf{U}(k-1)\mathbf{M}(k-1)\times\mathbf{U}(k)\mathbf{M}(k)\mathbf{U}(k)\mathbf{M}(k)=\mathbf{M}(k-1), \tag{A9}$$

which proves by mathematical induction Eq. (A7).

On the other hand, given that all GFC start with a hopping integral t_A,

$$\mathbf{M}_L(k)=\begin{pmatrix}0 & -t/t_A\\ 1 & 0\end{pmatrix}, \tag{A10}$$

and for the right side we have

$$\mathbf{M}_R(k)=\begin{pmatrix}0 & -\dfrac{[1-(-1)^k]t_B+[1+(-1)^k]t_A}{2t}\\ 1 & 0\end{pmatrix}. \tag{A11}$$

Therefore,

$$\tau_{i,j}=[\mathbf{M}_{\mathrm{R}}(k)\mathbf{M}(k)\mathbf{M}_{\mathrm{L}}(k)]_{i,j}=(-1)^i(1-\delta_{i,j}). \tag{A12}$$

Appendix B For the bond problem and a Hamiltonian of single s-band with real hopping integrals ($t_{j,j+1}=t_{j+1,j}<0$) like Eq. (1), the stationary Schrödinger equation ($\hat{H}\Psi=E\Psi$) can be rewritten as $t_{j,j+1}C_{j+1}+t_{j,j-1}C_{j-1}=EC_j$, or in the matrix form as

$$\begin{pmatrix}C_{j+1}\\ C_j\end{pmatrix}=\mathbf{T}_j\begin{pmatrix}C_j\\ C_{j-1}\end{pmatrix}=\begin{pmatrix}\dfrac{E}{t_{j,j+1}} & -\chi_j\\ 1 & 0\end{pmatrix}\begin{pmatrix}C_j\\ C_{j-1}\end{pmatrix}, \tag{B1}$$

where $\chi_j\equiv t_{j,j-1}/t_{j,j+1}$. For $E=0$ in a linear chain of two sites, the product of two transfer matrices [$\mathbf{M}(2)$] is

$$\mathbf{M}(2)\equiv\begin{pmatrix}0 & -\chi_j\\ 1 & 0\end{pmatrix}\begin{pmatrix}0 & -\chi_{j-1}\\ 1 & 0\end{pmatrix}=\begin{pmatrix}-\chi_j & 0\\ 0 & -\chi_{j-1}\end{pmatrix}. \tag{B2}$$

For the case of three sites we have

$$\mathbf{M}(3)=\begin{pmatrix}0 & -\chi_{j+1}\\ 1 & 0\end{pmatrix}\begin{pmatrix}-\chi_j & 0\\ 0 & -\chi_{j-1}\end{pmatrix}=\begin{pmatrix}0 & (-1)^2\chi_{j+1}\chi_{j-1}\\ -\chi_j & 0\end{pmatrix}. \tag{B3}$$

In general, if the number of atoms (N) is even,

$$\mathbf{M}(N)=\begin{pmatrix}(-1)^{N/2}\prod_{l=1}^{N/2}\chi_{2l} & 0\\ 0 & (-1)^{N/2}\prod_{l=1}^{N/2}\chi_{2l-1}\end{pmatrix}, \tag{B4}$$

while for N odd we have

$$\mathbf{M}(N)=\begin{pmatrix}0 & (-1)^{(N+1)/2}\prod_{l=1}^{(N+1)/2}\chi_{2l-1}\\ (-1)^{(N-1)/2}\prod_{l=1}^{(N-1)/2}\chi_{2l} & 0\end{pmatrix}. \tag{B5}$$

For a linear chain connected to two periodic semi-infinite leads, we have $t_{N,N+1}=t_{1,0}$ and then a unitary determinant [$\det|\mathbf{M}(N)|=1$]. Hence, the transmittance (T) at $E=0$ is

$$T(E=0)=\frac{4}{\left(m_{1,1}+m_{2,2}\right)^2+\left(m_{1,2}-m_{2,1}\right)^2}, \tag{B6}$$

being $m_{i,j}$ the elements of matrix $\mathbf{M}(N)$. In consequence, for the case of an even number N of atoms, the condition for a transparent state ($T=1$) is

$$\left(\prod_{l=1}^{N/2}\chi_{2l}+\prod_{l=1}^{N/2}\chi_{2l-1}\right)^2=4 \tag{B7}$$

and then

$$\prod_{l=1}^{N/2}\chi_{2l}+\prod_{l=1}^{N/2}\chi_{2l-1}=\frac{t_{2,1}t_{4,3}t_{6,5}\cdots t_{N,N-1}}{t_{2,3}t_{4,5}t_{6,7}\cdots t_{N,N+1}}+\frac{t_{1,0}t_{3,2}t_{5,4}\cdots t_{N-1,N-2}}{t_{1,2}t_{3,4}t_{5,6}\cdots t_{N-1,N}}=2. \tag{B8}$$

Let us define the first term in Eq. (B8) as x and then

$$x+\frac{1}{x}=2, \tag{B9}$$

which leads to the unique physical solution of $x=1$. Therefore, the condition of transparent state is

$$\prod_{l=1}^{N/2}t_{2l,2l-1}=\prod_{l=1}^{N/2}t_{2l,2l+1}. \tag{B10}$$

On the other hand, if N is odd, the transparent state appears only if

$$\left[\prod_{l=1}^{(N+1)/2}\chi_{2l-1}+\prod_{l=1}^{(N-1)/2}\chi_{2l}\right]^2=4, \tag{B11}$$

i.e.,

$$\prod_{l=1}^{(N+1)/2}\chi_{2l-1}+\prod_{l=1}^{(N-1)/2}\chi_{2l}=\frac{t_{1,0}t_{3,2}t_{5,4}t_{7,6}}{t_{1,2}t_{3,4}t_{5,6}t_{7,8}}\cdots\frac{t_{N,N-1}}{t_{N,N+1}}+\frac{t_{2,1}t_{4,3}t_{6,5}t_{8,7}}{t_{2,3}t_{4,5}t_{6,7}t_{8,9}}\cdots\frac{t_{N-1,N-2}}{t_{N-1,N}}=2. \tag{B12}$$

Using again that $t_{1,0}=t_{N,N+1}$ and defining the second term of Eq. (B12) as y, we obtain

$$\frac{1}{y}+y=2\Rightarrow y=1. \tag{B13}$$

Equation (B13) implies the same result that for the even N case, i.e.,

$$\prod_{l=1}^{(N-1)/2}\gamma_{2l}=1\Rightarrow\prod_{l=1}^{(N-1)/2}t_{2l,2l-1}=\prod_{l=1}^{(N-1)/2}t_{2l,2l+1}. \tag{B14}$$

Condition (B10) or (B14) is fully satisfied, for example, if the system is composed by segments and each of them has an even number of bonds.

Appendix C The transmittance (T) of an infinite periodic chain with hopping integral t and a single site impurity of self-energy $\varepsilon_{\rm imp}$ is [24]

$$T(\mu)=\frac{4-(\mu/t)^2}{4-(\mu/t)^2+(\varepsilon_{\rm imp}/t)^2}. \tag{C1}$$

For the case of a periodic chain with a coupled Fano impurity chain as shown in Fig. 12, $\varepsilon_{\rm imp}$ in Eq. (C1) is replaced by the continued fraction $\alpha_{N_F}(\mu)$, which can be obtained from the recursive relation

$$\alpha_N(\mu)=\frac{t_N^2}{\mu-\alpha_{N-1}(\mu)} \tag{C2}$$

with $\alpha_1(\mu)=t_1^2/\mu$. Defining

$$\beta_N(\mu)\equiv\det\begin{pmatrix}\mu & -t_1 & 0 & \cdots & 0\\ -t_1 & \mu & -t_2 & \ddots & \vdots\\ 0 & -t_2 & \mu & \ddots & 0\\ \vdots & \ddots & \ddots & \ddots & -t_{N-1}\\ 0 & \cdots & 0 & -t_{N-1} & \mu\end{pmatrix} \tag{C3}$$

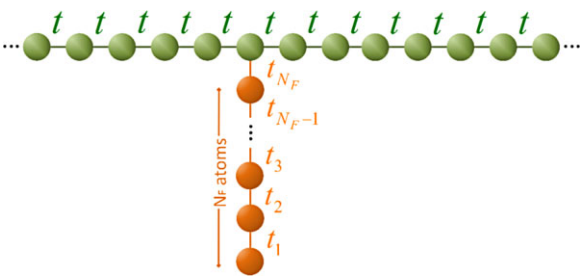

Figure 12 Schematic representation of an infinite periodic chain with a Fano impurity chain of N_F atoms

and calculating the determinant using expansion by minors, we have

$$\beta_N(\mu)=\mu\beta_{N-1}(\mu)-t_{N-1}^2\beta_{N-2}(\mu). \tag{C4}$$

From Eqs. (C2) and (C3) we obtain $\alpha_2(\mu)=t_2^2\beta_1(\mu)/\beta_2(\mu)$. Let us assume that

$$\alpha_N(\mu)=\frac{t_N^2\beta_{N-1}(\mu)}{\beta_N(\mu)}. \tag{C5}$$

Hence, using Eq. (C2), (C4) and (C5) we have

$$\begin{aligned}\alpha_{N+1}(\mu)&=\frac{t_{N+1}^2}{\mu-\alpha_N(\mu)}=\frac{t_{N+1}^2\beta_N(\mu)}{\mu\beta_N(\mu)-t_N^2\beta_{N-1}(\mu)}\\&=\frac{t_{N+1}^2\beta_N(\mu)}{\beta_{N+1}(\mu)},\end{aligned} \tag{C6}$$

which proves the relation (C5) by mathematical induction. Therefore, the transmittance of an infinite periodic chain with a finite Fano impurity chain of N_F atoms becomes

$$T(\mu)=\frac{4-(\mu/t)^2}{4-(\mu/t)^2+\left[\frac{t_{N_F}^2\beta_{N_F-1}(\mu)}{t\beta_{N_F}(\mu)}\right]^2}. \tag{C7}$$

Notice that there are transparent states with $T(\mu)=1$ when $\beta_{N_F-1}(\mu)=0$, which occur at the eigenvalues of a chain formed by hopping integrals $t_1,t_2,\cdots,$ and t_{N_F-2}.

Acknowledgements This work has been partially supported by UNAM-IN113813, UNAM-IN113714 and CONACyT-131596. One of the authors (C.?R.) thanks to the Program of Post-Doctoral Scholarships in the UNAM. Computations were performed at Miztli of DGTIC-UNAM.

References

[1] E. Abrahams, P. W. Anderson, D. C. Licciardello, and T. V. Ramakrishnan, Phys. Rev. Lett. **42**, 673 (1979).
[2] E. Abrahams, S. V. Kravchenko, and M. P. Sarachik, Rev. Mod. Phys. **73**, 251 (2001).
[3] S. V. Kravchenko and M. P. Sarachik, Rep. Prog. Phys. **67**, 1 (2004).
[4] W. R. Clarke, C. E. Yasin, A. R. Hamilton, A. P. Micolich, M. Y. Simmons, K. Muraki, Y. Hirayama, M. Pepper, and D. A. Ritchie, Nature Phys. **4**, 55 (2008).
[5] J. C. Flores, J. Phys.: Condens. Matter **1**, 8471 (1989).
[6] G. Hui-Fen and T. Rui-Bao, Commun. Theor. Phys. **46**, 929 (2006).
[7] X. Q. Huang, S. S. Jiang, R. W. Peng, Y. M. Liu, F. Qiu, and A. Hu, Mod. Phys. Lett. B **17**, 1461 (2003).
[8] R. Oviedo-Roa, L. A. Pérez, and C. Wang, Phys. Rev. B **62**, 13805 (2000).
[9] D. H. Dunlap, H.-L. Wu, and P. W. Phillips, Phys. Rev. Lett. **65**, 88 (1990).

[10] D. Damanik and A. Gorodetski, Israel J. Math., DOI: 10.1007/s11856-014-1108-x (2014).
[11] E. Maciá, ISRN Condens. Matter Phys. **2014**, 165943 (2014).
[12] S. Thiem and M. Schreiber, Phys. Rev. B **85**, 224205 (2012).
[13] E. Maciá, Aperiodic Structures in Condensed Matter (Taylor & Francis, New York, 2009).
[14] Z. Zhang, P. Tong, J. Gong, and B. Li, Phys. Rev. E **83**, 056205 (2011).
[15] H. Barghathi, D. Nozadze, and T. Vojta, Phys. Rev. E **89**, 012112 (2014).
[16] B. Kramer and A. MacKinnon, Rep. Prog. Phys. **56**, 1469 (1993).
[17] V. Sánchez and C. Wang, Phys. Rev. B **70**, 144207 (2004).
[18] Y. Imry and R. Landauer, Rev. Mod. Phys. **71**, S306 (1999).
[19] C. Ramírez and V. Sánchez, Phys. Status Solidi A **210**, 2431 (2013).
[20] A. Ron and Y. Dagan, Phys. Rev. Lett. **112**, 136801 (2014).
[21] J. M. Luck, C. Godreche, A. Janner, and T. Janssen, J. Phys. A, Math. Gen. **26**, 1951 (1993).
[22] J. Moon, J.-H. Kim, Z. C. Y. Chen, J. Xiang, and R. Chen, Nano Lett. **13**, 1196 (2013).
[23] J. Zhu, H. Peng, A. F. Marshall, D. M. Barnett, W. D. Nix, and Y. Cui, Nature Nanotechnol. **3**, 477 (2008).
[24] V. Sánchez, C. Ramírez, F. Sánchez, and C. Wang, Physica B **449**, 121 (2014).